

(12) LEVEL III

AD-E430 463

AD

ADA 086106

MEMORANDUM REPORT ARBRL-MR-03018

WINDOWED CHAMBER INVESTIGATION OF
THE BURNING RATE OF LIQUID
MONOPROPELLANTS FOR GUNS

William F. McBratney

April 1980

DTIC
ELECTE
S JUL 2 1980 D
B



US ARMY ARMAMENT RESEARCH AND DEVELOPMENT COMMAND
BALLISTIC RESEARCH LABORATORY
ABERDEEN PROVING GROUND, MARYLAND

DDC FILE COPY

Approved for public release; distribution unlimited.

80 6 18 0 13

Destroy this report when it is no longer needed.
Do not return it to the originator.

Secondary distribution of this report by originating
or sponsoring activity is prohibited.

Additional copies of this report may be obtained
from the National Technical Information Service,
U.S. Department of Commerce, Springfield, Virginia
22151.

The findings in this report are not to be construed as
an official Department of the Army position, unless
so designated by other authorized documents.

*The use of trade names or manufacturers' names in this report
does not constitute endorsement of any commercial product.*

UNCLASSIFIED

SECURITY CLASSIFICATION OF THIS PAGE (When Data Entered)

REPORT DOCUMENTATION PAGE		READ INSTRUCTIONS BEFORE COMPLETING FORM
1. REPORT NUMBER	2. GOVT ACCESSION NO.	3. RECIPIENT'S CATALOG NUMBER
MEMORANDUM REPORT AKSR1-MR-03013 -1 AD-A096106		
4. TITLE (and Subtitle)		5. TYPE OF REPORT & PERIOD COVERED
Windowed Chamber Investigation of the Burning Rate of Liquid Monopropellants for Guns		Final
7. AUTHOR(s)		6. PERFORMING ORG. REPORT NUMBER
William F. McBratney		
9. PERFORMING ORGANIZATION NAME AND ADDRESS		8. CONTRACT OR GRANT NUMBER(s)
US Army Ballistic Research Laboratory ATTN: DRDAR-BLP Aberdeen Proving Ground, MD 21005		
10. PROGRAM ELEMENT, PROJECT, TASK AREA & WORK UNIT NUMBERS		
1L161102AH43		
11. CONTROLLING OFFICE NAME AND ADDRESS		12. REPORT DATE
US Army Armament Research and Development Command US Army Ballistic Research Laboratory ATTN: DRDAR-BL Aberdeen Proving Ground, MD 21005		April 1980
14. MONITORING AGENCY NAME & ADDRESS (if different from Controlling Office)		13. NUMBER OF PAGES
		48
		15. SECURITY CLASS. (of this report)
		Unclassified
		16. DECLASSIFICATION/DOWNGRADING SCHEDULE
16. DISTRIBUTION STATEMENT (of this Report)		
Approved for public release; distribution unlimited.		
17. DISTRIBUTION STATEMENT (of the Abstract entered in Block 20, if different from Report)		
18. SUPPLEMENTARY NOTES		
19. KEY WORDS (Continue on reverse side if necessary and identify by block number)		
Liquid Propellant, Burning Rate, surface stability, photographic, NOS-365, OTTO II, NOSET "A"		
20. ABSTRACT (Continue on reverse side if necessary and identify by block number)		
<p>d11</p> <p>Equipment and techniques have been developed for the photographic observation of burning liquid monopropellants at pressures up to 200 MPa. Many details of the liquid surface and the reaction zone above it may be observed. Preliminary photographic runs have been made on OTTO Fuel II, NOS-365, and NOSET "A".</p>		

TABLE OF CONTENTS

	Page
LIST OF ILLUSTRATIONS.	5
I. INTRODUCTION	7
II. BACKGROUND	7
III. APPARATUS AND EQUIPMENT.	8
IV. EXPERIMENTAL	8
A. NOS-365 -- Polypropylene Straws, Gelled.	8
B. Hot Wall Effects	12
C. NOS-365, H37, 2% Kelzan.	12
D. NOS-365, H37, Not Gelled	19
E. OTTO Fuel II	19
F. NCSET "A".	39
V. CONCLUSIONS.	39
DISTRIBUTION LIST.	45

ACCESSION for		
NTIS	White Section	<input checked="" type="checkbox"/>
DDC	Buff Section	<input type="checkbox"/>
UNANNOUNCED		<input type="checkbox"/>
JUSTIFICATION _____		
BY _____		
DISTRIBUTION/AVAILABILITY CODES		
Dist.	AVAIL and/or	SPECIAL
A		-

LIST OF ILLUSTRATIONS

Figure	Page
1. NOS-365, H37, 2% Kelzan, 3 mm Polypropylene Straw, 20 MPa	9
2. NOS-365, H37, 2% Kelzan, 3 mm Polypropylene Straw, 42 MPa	10
3. NOS-365, H37, 2% Kelzan, 3 mm Polypropylene Straw, 62 MPa	11
4. NOS-365, H37, 2% Kelzan, 6.1 x 1.5 mm Acrylic Cell, 28.6 MPa	14
5. NOS-365, H37, 2% Kelzan, 6.1 x 1.5 mm Acrylic Cell, 55 MPa	15
6. NOS-365, H37, 2% Kelzan, 6.1 x 1.5 mm Acrylic Cell, 124 MPa	16
7. NOS-365, H37, 2% Kelzan, 6.1 x 1.5 mm Acrylic Cell, 169 MPa	17
8. NOS-365, H37, 2% Kelzan, 6.1 x 1.5 mm Acrylic Cell, 195 MPa	18
9. NOS-365, H37 Data Plot, 2% Kelzan	20
10. NOS-365, H37, Not Gelled, 6.1 x .95 mm Glass Cell, 29 MPa	22
11. OTTO Fuel II, 3.2 x .95 mm Glass Cell, 8.4 MPa, (Meniscus)	23
12. OTTO Fuel II, 6.1 x 1.5 mm Acrylic Cell, 10.3 MPa (Fuse Wire)	25
13. OTTO Fuel II, 3.2 x .95 mm Glass Cell, 41.4 MPa	26
14. OTTO Fuel II, 6.1 x .95 mm Glass Cell, 47 MPa, (Sloshing)	27
15. OTTO Fuel II, 6.0 x 1.5 mm Acrylic Cell, 62 MPa	29
16. OTTO Fuel II, 6.0 x 1.5 mm Acrylic Cell, 82.7 MPa	32
17. OTTO Fuel II, 6.1 x 1.5 mm Acrylic Cell, 129 MPa	34

LIST OF ILLUSTRATIONS (Cont'd)

Figure	Page
18. OTTO Fuel II, 6.1 x 1.5 mm Acrylic Cell, 156 MPa	36
19. Burn Rates for OTTO Fuel II	38
20. NOSET "A", 6.0 x .95 mm Glass Cell, 20 MPa	40
21. NOSET "A", 6.0 x 1.5 mm Acrylic Cell, 69.6 MPa	42

I. INTRODUCTION

In conjunction with a program to control and model the combustion of liquid monopropellants in guns, an effort has been made to determine the pressure dependent burning rate of several liquid monopropellants. Previous work was directed at utilizing more or less standard strand burner type techniques -- straws, gellation, ignition techniques.¹

The present report covers some work performed in a windowed chamber to confirm previous results and to identify causes of erratic results and non-planar combustion.

II. BACKGROUND

In order to provide a basis for testing and comparing candidate liquid monopropellants for gun use, it was desired to determine combustion rates as a function of pressure.

The initial effort was directed at measuring the burning rate in plastic straws filled with the monopropellants. Data reproducibility and diameter independence were used as crude tests of the planarity of the burning surface in order to develop ignition and shielding techniques.¹ Gellation was necessary in order to produce stable results with one of the candidate propellants.

The lower pressure work with gelled NOS-365 gave data points with appreciable scatter. Inspection of the straw remnants showed signs of decreased thermal output at the lower pressures. The preliminary interpretation of these data was that the propellant was decomposing at a relatively low temperature and therefore not melting the straw out of the way in a consistent manner.

Considering the ease with which a liquid surface may be deformed and the necessarily larger apparent burn rate associated with an increased surface area, improved techniques for determining the surface shape were desired.

Interaction of the propellant with its container and the ignition source provide disturbances that will initially alter the surface from a planar shape. Techniques for minimizing these disturbances and studying the duration of the disturbance were desired.

¹W. F. McBratney, R. Bensinger and W. Arford, "Strand Combustion Rates for Some Liquid Monopropellants at Gun Functioning Pressures," BRL Memorandum Report No. 2658, Aug 76. (AD#B013130L)

III. APPARATUS AND EQUIPMENT

A windowed chamber capable of operating at pressures up to 200 MPa was obtained and set-up for use in connection with the pressurization apparatus of the BRL strand burner facility.

The chamber has a 15 cm interior diameter and allows a 10 cm optical path between the windows which are attached to the end plugs. The end plugs are provided with plates which may be altered to provide different apertures. Those apertures used in this series of tests ranged from 6 mm to 13 mm wide by 37 mm long.

A quartz-halogen lamp was used to back light the samples through a diffuser screen placed within the chamber and near the sample.

A Fastax half frame 16 mm camera operating at approximately 1100 frames per second was used for most of the tests in this report. Ektachrome 7242 film was normally used.

The samples of liquid propellant were held in polypropylene straws or in special cells. These cells were of rectangular cross-section and designed like spectroscopy cells. Various cell window and spacer materials were tested. Glass microscope slides worked well for some of the tests but tended to shatter if the combustion was not stable. Acrylic sheet generally gave satisfactory results as far as remaining together but would interact with the OTTO Fuel II if the photographic lights were left on too long, causing an apparent gel layer to form.

Ignition was achieved by contact with a heated nichrome wire.

IV. EXPERIMENTAL

A. NOS-365 -- Polypropylene Straws, Gelled

One of the observations made during the lower pressure strand burner runs with NOS-365 was that below ~ 20 MPa stringy fragments of the polypropylene were left after the burn. As pressures were decreased further the portion of the straw remaining increased in size. At sufficiently low pressures, most of the straw remained but was thermally distorted and collapsed. At even lower pressures the straw was not even distorted.

With a marginal heat release from the propellant, the melting of the polypropylene is probably not consistent. This may account for the scatter in the low pressure data.

Figures 1, 2, and 3 show straws during the burn cycle at pressures of 20 MPa, 42 MPa and 62 MPa, respectively. In Figure 1 at 20 MPa, the

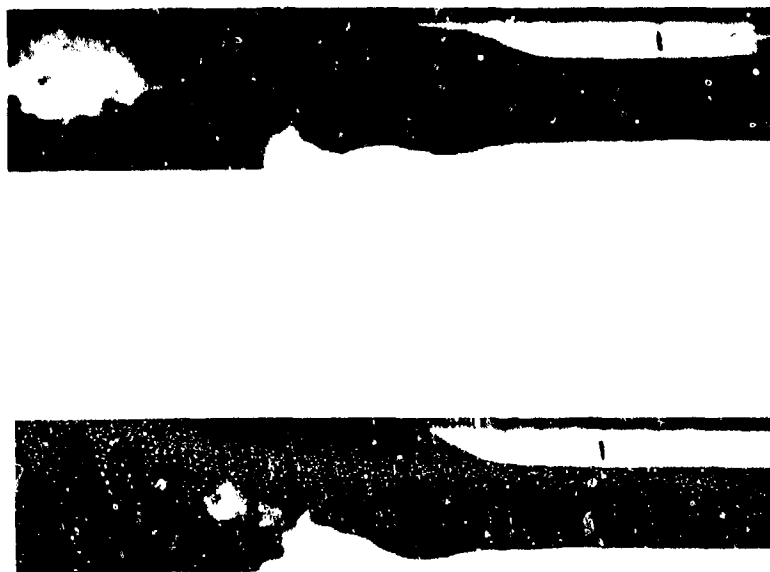


Figure 1. NOS-365, H37, 2% Kelzan, 3 mm Polypropylene Straw, 20 MPa

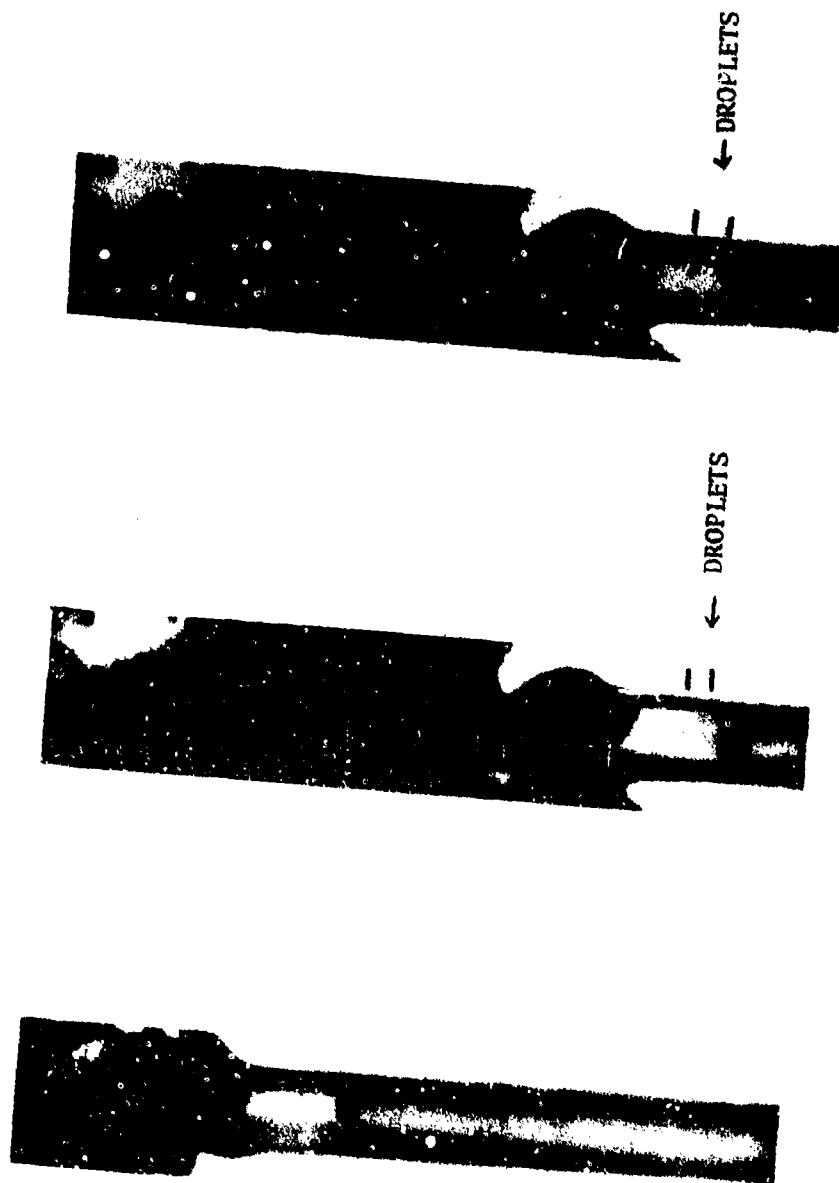


Figure 2. NOS-365, H37, 2% Kelzan, 3 mm Polypropylene Straw, 42 MPa



Figure 3. NOS-365, H37, 2% Kelzan, 3 mm Polypropylene Straw, 62 MPa

straw appears to melt and collapse but not burn off. In the left frame, the formation of a bulbous zone is observed. The top of the straw appears to have collapsed inward, giving a restricted orifice. As the burn progresses, the length of the straw remnant above the burn surface increases (Figure 1, left, ~ 10 mm; Figure 1, right, ~ 13 mm).

In Figures 2 and 3, the top of the straw is roughly 7 mm above the burn front but the higher pressure run in Figure 3 appears to give a more uniform burn-off with less of the melt thickening observed in Figure 1.

These figures confirm the suspicion that at the lower pressures the melting of the straw may give erratic data in the standard strand burner apparatus, where the melting of the fuze wire will be dependent upon the melting away of the straw to allow the hot gas to contact the wire.

In Figure 2, the two frames at the right show a droplet being ejected from the burn zone.

B. Hot Wall Effects

Observation of the non-planar burning of these propellants in rectangular cross section cells reveals one of the mechanisms for high mass burning rates. As the wave-like sloshing of the propellant from one side of the cell to the other occurs, the cell walls in areas that were previously uncovered have become heated. When the propellant is driven back into this region by the wave action, the hot walls react with the propellant, forcing the propellant away from the wall. This produces a relatively large propellant surface area. The films of this effect show what appears to be a jetting action of the propellant into the gas zone.

This clipping of the rising portion of the wave may contribute to the high mass burn rate in at least two ways. The material thrown away from the hot walls has a high mass burning rate due to the increased surface area and is rapidly eliminated from participating in the wave action. This eliminates the material from participating in "normal" stabilizing mechanisms. In addition, the high local mass burning rate will produce a localized surge in pressure to add to the destabilizing mechanisms. So far, it has been difficult to obtain films of this hot wall effect that are good enough to reproduce a plate illustration.

C. NOS-365, H37, 2% Kelzan

1. Lower Pressures. Observations on NOS-365 in the transparent cells at pressures of 55 MPa and below show a red zone above the burn front and ejecta (small droplets) exiting the cell.

The red zone above the burn front at 28 MPa has the appearance of a flame of small height, however, at 55 MPa, the red zone has disappeared and the burn zone appears to be an opaque, non-luminous layer. From these data and observations on NOS-365 without gellation, it is probable that the red zone is caused by NO_2 from the decomposition reaction. Red-brown fumes are observed at atmospheric pressure, and it is probable that this red zone corresponds to these fumes.¹

At pressures near atmospheric the decomposition of the NOS-365 proceeds into the propellant while generating froth. At higher pressures the froth does not form a growing layer but apparently the liquid from the froth reaction collects on the reaction front and is blown away as droplets. These droplets are readily seen in films taken of the reaction near 28 MPa (Figure 4).

The films taken at 28 MPa and 55 MPa (Figure 5) show reactions that start off with relatively flat, horizontal surfaces. As the reaction proceeds, the surface becomes tilted relative to the horizontal. This may result in a relatively simple tilted surface as at 28 MPa (Figure 4) or a convex surface consisting largely of two simple tilted portions as at 55 MPa (Figure 5). These observations correlate with the observations that the burn surface is convex (\sim conical) at these pressures in polypropylene straws.

A probable explanation of the mechanism which causes the convex burn surface at these lower pressures, is given by the observation that NOS-365 appears to react in a hypergolic manner with the liquid remnant from the fizz reaction.¹ As this remnant liquid is ejected from the burn front some of it will hit the walls of the test cell and be returned to the reaction area along the cell walls causing a higher reaction rate near the walls.

2. Higher Pressures. Photographic runs covering the pressure range of 100 MPa to 195 MPa show a relatively stable burn surface. The ignition event or the deformity of the initial surface provide early burn surfaces which generally approach a flat, horizontal shape as the burn progresses down the sample.

Figures 6 and 7 (124 MPa and 169 MPa) show more typical burns at high pressure, in which the ignition occurs near one edge of the sample. This causes one edge to lead the other for the early part of the burn, but the surface becomes flat within 0.25 mm across the width of the sample fairly early in the burn cycle.

In Figure 8 (195 MPa), the sample surface has a large depression near one side. During the ignition event, the flame propagates into this depression, producing a large initial deviation from planarity in the burn surface. The surface does not approach planarity until all but the bottom one centimeter of the sample has burned away.

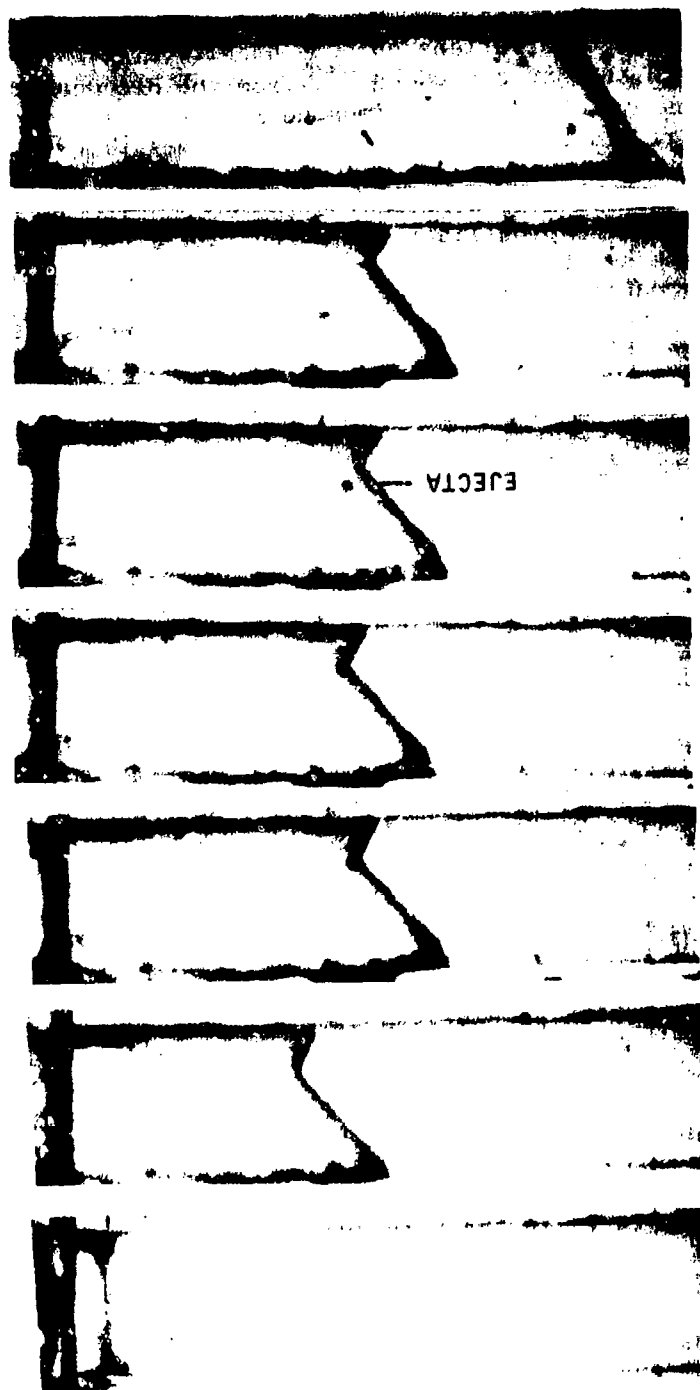


Figure 4. NOS-365, H37, 2% Kelzan, 6.1 x 1.5 mm Acrylic Cell, 28.6 MPa

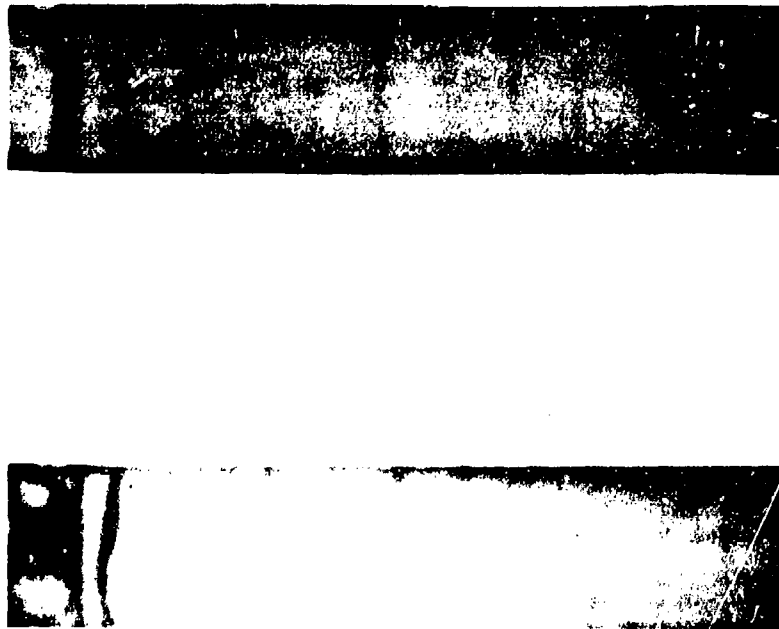


Figure 5. NOS-365, H37, 2% Kelzan, 6.1 x 1.5 mm Acrylic Cell, 55 MPa

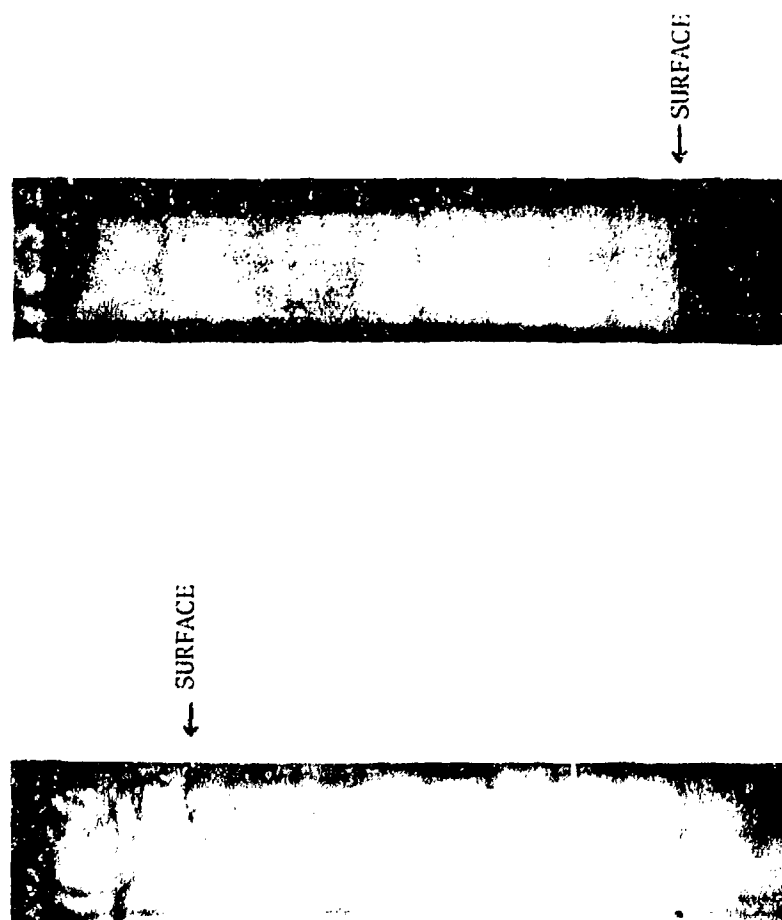


Figure 6. NOS-365, H37, 2% Kelzan, 6.1 x 1.5 mm Acrylic Cell, 124 MPa

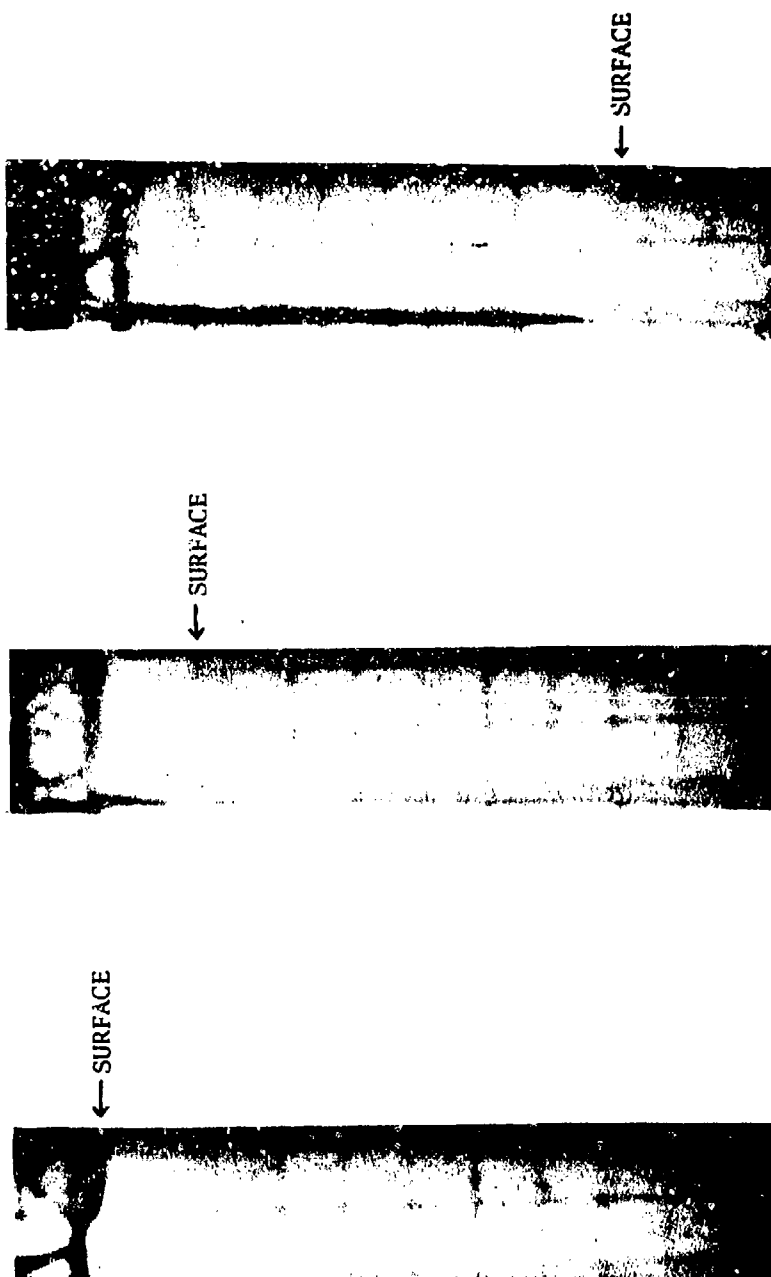


Figure 7. NOS-365, H37, 2% Kelzan, 6.1 x 1.5 mm Acrylic Cell, 169 MPa

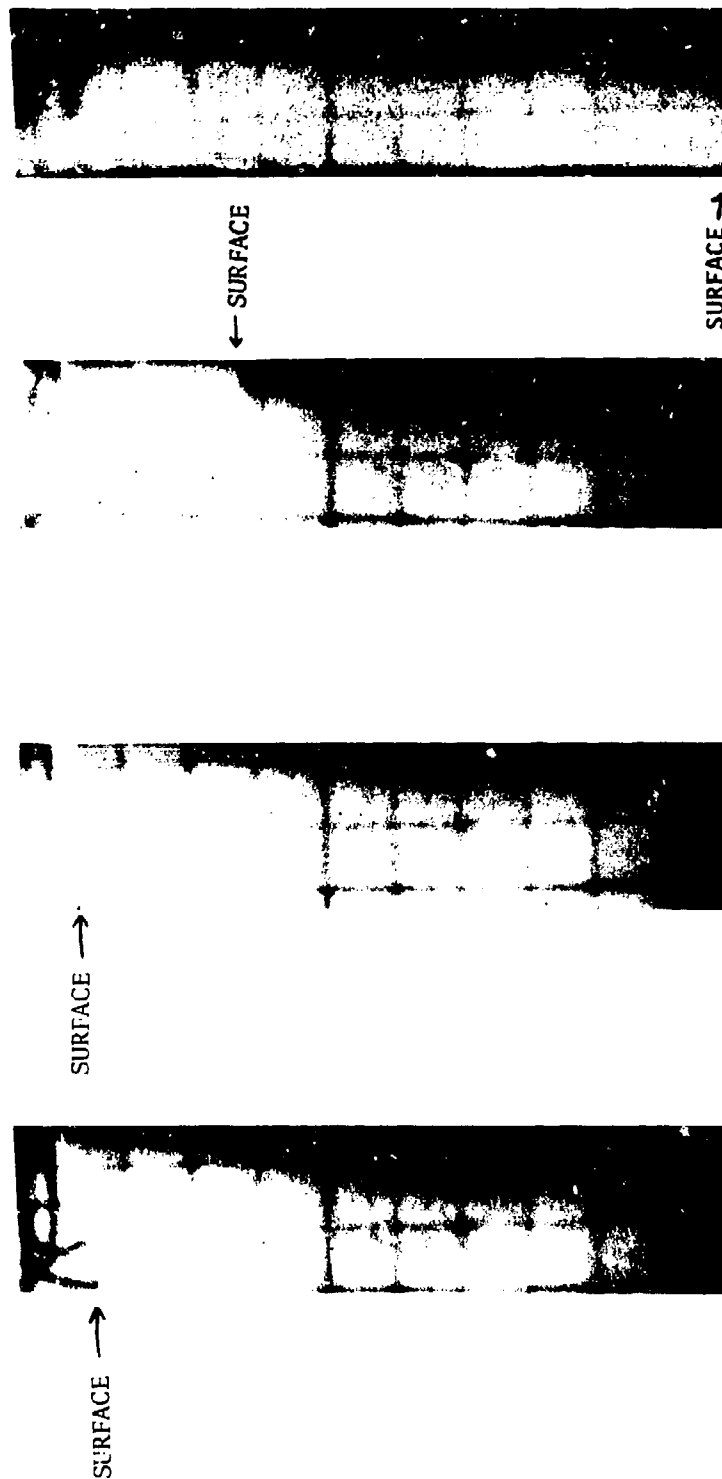


Figure 8. NOS-365, H37, 2% Kelzan, 6.1 x 1.5 mm Acrylic Cell, 195 MPa

3. Luminosity. In these gelled propellant tests the runs at the lower pressures do not appear to have luminous areas within the cells. At pressures of 100 MPa and above there appears to be a generalized low level of luminosity within the sample cell. All of the cell volume above the propellant sample appears slightly luminous at 195 MPa. The luminosity is softly reddish at 195 MPa. Any luminosity is at least an order of magnitude less than is observed with a 0.25 mm thick sample of M8 solid propellant.

At these higher pressures there generally occurs a flash of luminosity above the cell during the ignition phase. This luminosity occurs around the igniter wire.

4. Results. The data obtained from the photographic runs with NOS-365, H37, 2% Kelzan are plotted in Figure 9 and given in Table I. A reference line for the high pressure region has been taken from Ref. 1 for NOS-365, H6, 1.5% Kelzan. The data for the 2% gelled material falls consistently below that for the 1.5% gel concentration at the higher pressures. Data on the 2% material of the same propellant lot is being prepared for publication.

D. NOS-365, H37, Not Gelled

Figure 10 shows NOS-365, H37 in a glass cell at 29 MPa. The initial frame clearly shows the initial surface curvature and the immersion of the ignition wire. The following frames clearly show a small wave traveling to the right and eventually forming a jet up the wall. Numerous ejecta droplets are observed in this sequence.

E. OTTO Fuel II

1. Low Pressures. At pressures up to the neighborhood of 10 MPa stable surface curvature is observed during the burn. Apparently this is due to the surface tension of the liquid to cell contact. Figure 11 shows the curvature of the front in a glass cell at 8.4 MPa. It appears that the surface curvature decreases as the pressure is increased but the data is effected by the different cell materials used.

Crude calculations, based on the visible curvature of the front in glass cells in which the increased area is accounted for, give burning rates which are "close" to those obtained in the strand burner.

During some of the runs at lower pressures with acrylic cells, some anomalous low uncorrected rate data were obtained. Investigation led to the conclusion that OTTO Fuel II may be gelled with acrylic plastic. Under normal room conditions, acrylic will dissolve in OTTO Fuel II at a very low rate. However, when exposed to a photo-flood light or a source of heat, an increase of viscosity and finally gellation are fairly rapidly noted. [Test conditions were a thin layer of OTTO Fuel II on a sheet of acrylic].

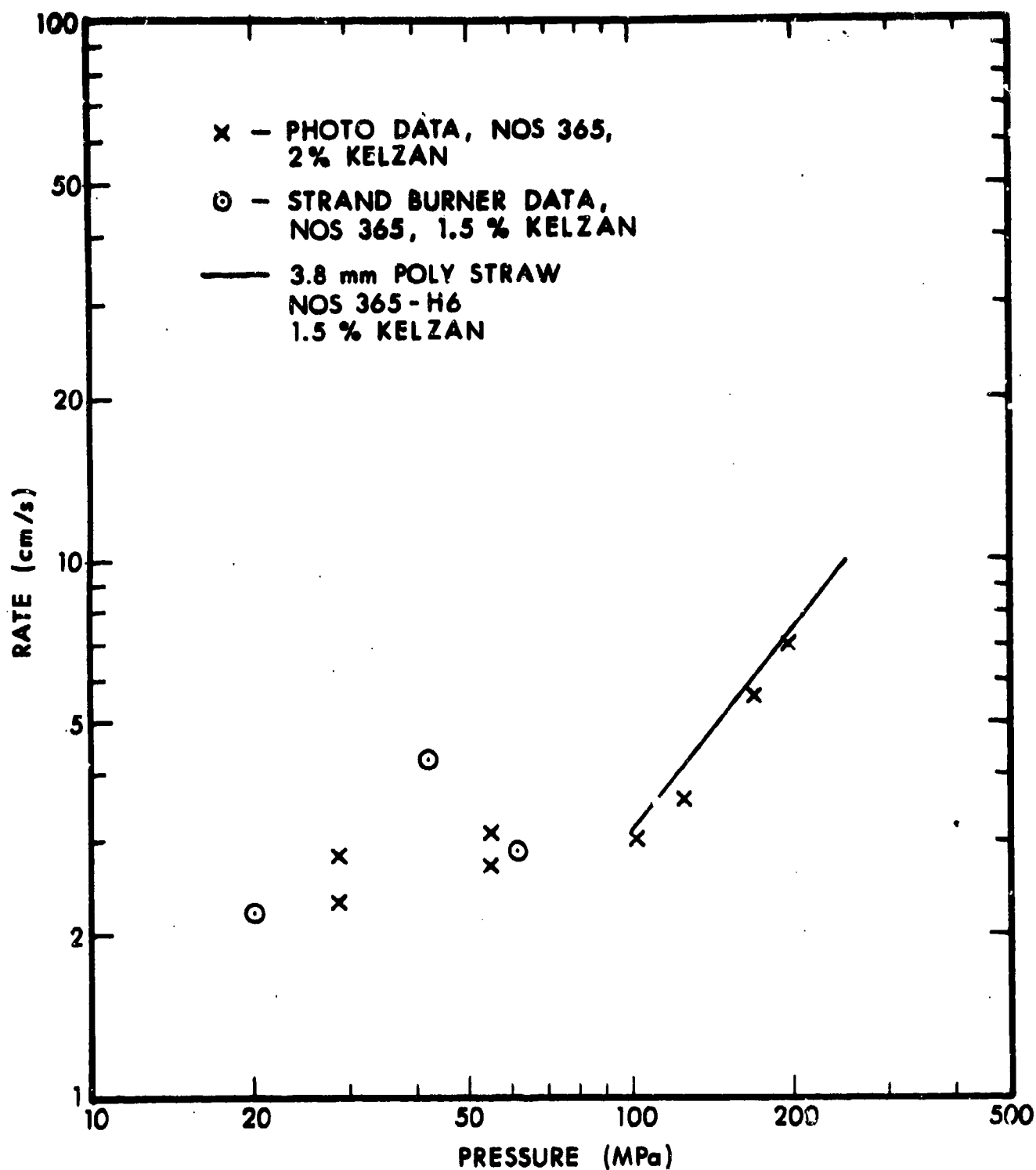
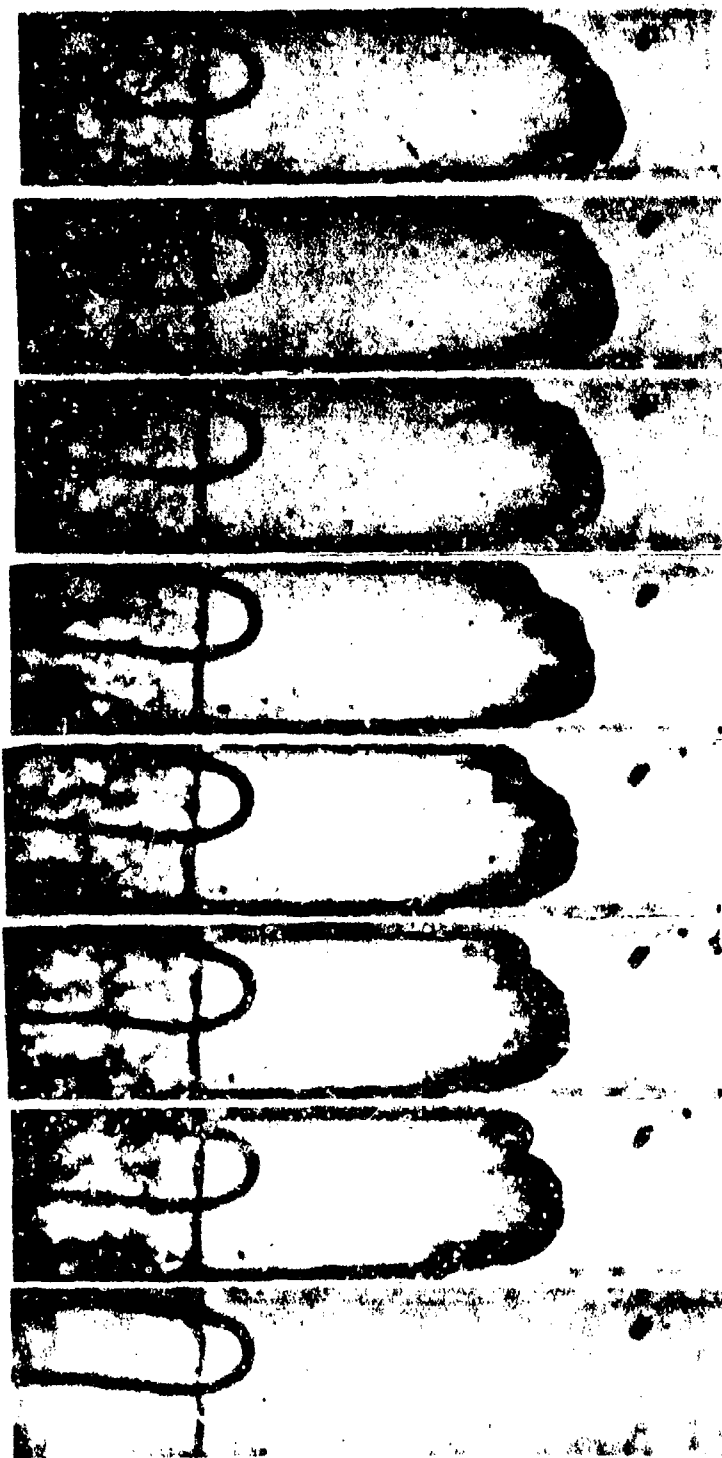


Figure 9. NOS-365, H37 Data Plot, 2% Kelzan

Table I. NCS-365, H37, 2% Kelzan

<u>P</u> MPa	<u>R</u> cm/s	<u>COMMENT</u>
20	2.17	3 mm polypropylene straw
42	4.24	3 mm polypropylene straw
62	2.87	3 mm polypropylene straw
196	6.97	6.1 x 1.5 mm cell Acrylic
169	5.55	6.1 x 1.5 mm cell Acrylic
124	3.59	6.1 x 1.5 mm cell Acrylic
102	3.0	6.1 x 1.5 mm cell Acrylic
55	2.7-3.1	6.1 x 1.5 mm Non-Planar Burn
28.6	2.3-2.8	6.1 x 1.5 mm Non-Planar Burn

NOTE: Estimated reading errors of 1% to 5% are to be expected from the photographic data. This is dependent upon the photographic quality and the nature of the surface.



BEFORE
IGNITION

$\Delta T = 3.6 \text{ ms}$

Figure 10. NOS-365, H37, Not Gelled, 6.1 x .95 mm Class Cell, 29 MPa



Figure 11. OTTO Fuel II, 3.2 x .95 mm Glass Cell, 8.4 MPa, (Meniscus)

During some of the pressure runs with thin acrylic cells the full intensity of the photographic lights was used during adjustment of the camera and mirrors. This was apparently enough to allow the propellant to dissolve some of the acrylic of the cell walls. Later tests were conducted with the light intensity reduced until the actual photographic run was started.

The information that the viscosity of OTTO Fuel II may be increased drastically by the solution of acrylic plastic should be of use in studying the stability of the combustion at higher pressures. Acrylic may be utilized as a gelling agent to modify the surface instabilities.

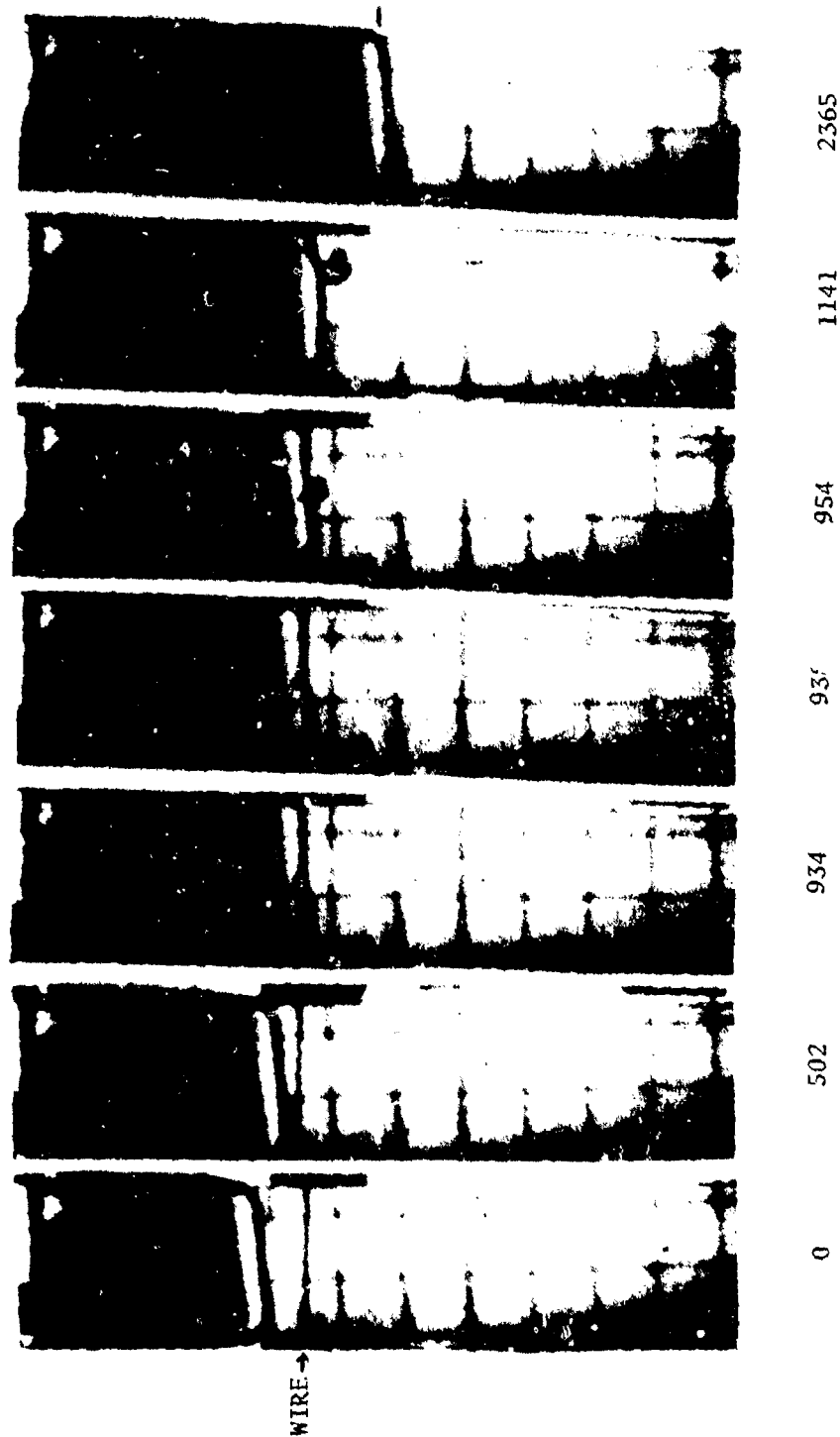
Figure 12 shows the progression of a burn front at 10.3 MPa over a piece of submerged fuse wire. The cell is acrylic. In this pressure range at least, this plate shows that relatively large disturbances may be imposed upon the burning surface and the surface will stabilize itself.

2. Mid-Pressure Range. The pressure range of 10 MPa to approximately 40 MPa (Figure 13) covers the transition from surface tension stabilization to a relatively flat burn surface with small scale disturbances becoming evident at the higher values.

3. Higher Pressures. In the pressure region above 40 MPa, strongly non-planar burning has been obtained with the techniques employed to this date. In these tests the initial surface has been non-planar (surface tension) and the ignition event has been vigorous enough to strongly drive the surface in localized areas.

At 46.9 MPa (Figure 14), slightly asymmetric ignition initiates a strong, sloshing type of wave action. The sequence of photos illustrates this motion starting at the point on the right side of the cell when the meniscus has been reduced to a minimum by the vertical motion of the liquid. In the second frame, some liquid has moved further upward while being ignited along the walls by the previously heated glass walls. This ignition has driven the propellant away from the walls and towards the center line of the cell, thereby creating a jet of propellant up the cell. This will create a sudden change in surface area and thus pressure in this area which will act to stop the vertical motion of the liquid in this area and assist in driving the liquid back down in this region. The rest of the sequence of frames shows the dropping of the liquid with the resultant large meniscus of liquid on the right side of the cell and the corresponding upsurge of liquid on the left side of the cell (~ 9 ms between frames).

Figure 15 (62 MPa) shows the rapid growth of the ignition process and its development into an asymmetric shape. Of special interest in this sequence is the clear development of the burn front in the first few frames. Clearly a meniscus of liquid remains on the wall in both horizontal dimensions. The burn-off of this meniscus is clearly seen in later frames.



MILLISECONDS

Figure 12. OTTO Fuel II, 6.1 x 1.5 mm Acrylic Cell, 10.3 MPa (Fuse Wire)



Figure 13. OTTO Fuel II, 3.2 x .95 mm Glass Cell, 41.4 MPa



$\Delta T = 9 \text{ ms}$

Figure 14. OTTO Fuel II, 6.1 x .95 mm Glass Cell, 47 MPa, (Sloshing)



LATER

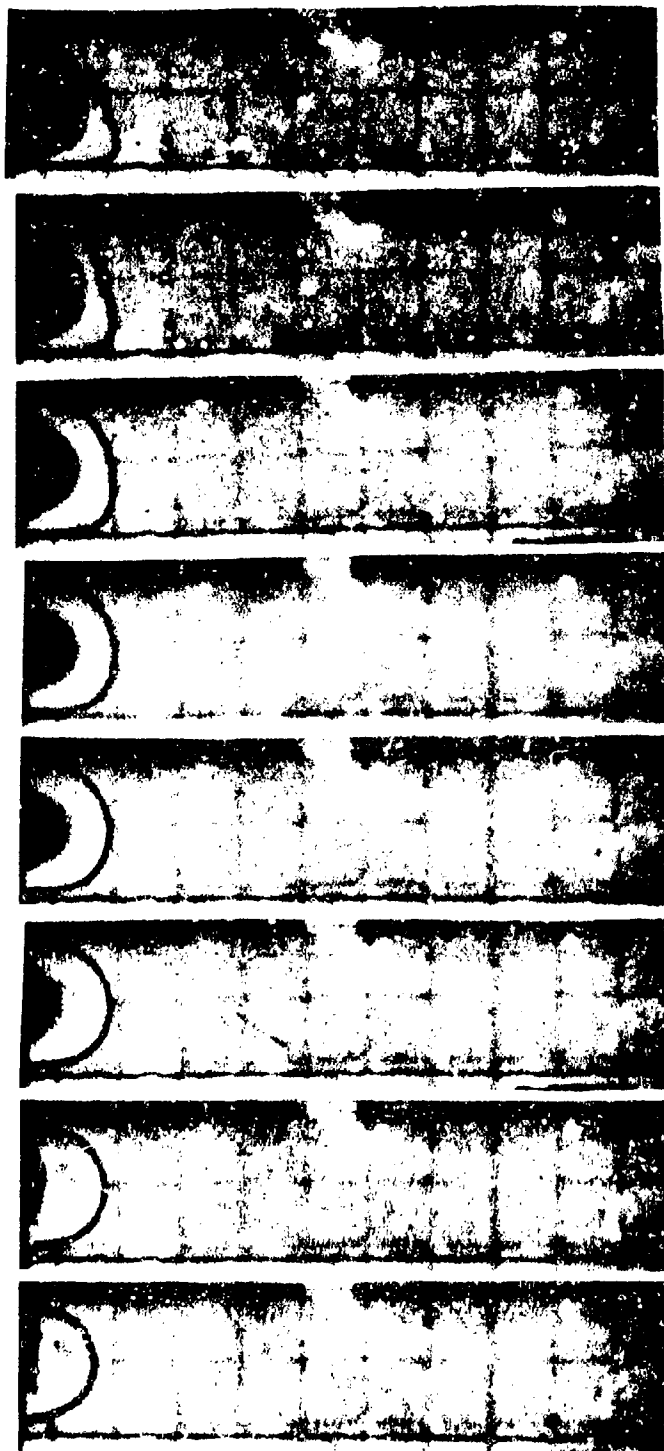
$\Delta T = 9 \text{ ms}$

Figure 14. OTTO Fuel II, 6.1 x .95 mm Glass Cell, 47 MPa, (Sloshing) (Cont'd)



$\Delta T = .9 \text{ ms}$

Figure 15. OTTO Fuel II, 6.0 x 1.5 mm Acrylic Cell, 62 MPa



$\Delta T = 1.8 \text{ ms}$

Figure 15. OTTO Fuel II, 6.0 x 1.5 mm Acrylic Cell, 62 MPa (Cont'd)

Figure 16 (82.7 MPa) shows another example of the sloshing motion. The last frames of the sequence again clearly show the burning off of a wall bound meniscus layer along the center of the cell.

The presence of a meniscus layer on the wall allows the liquid in the wave to rise up the cell to at least the extent of the meniscus due to its protection of the wall from the combustion gases.

Figure 17 shows OTTO Fuel II in an acrylic cell at 129 MPa. This burn starts out strongly asymmetric due to the liquid leaking out so that a major portion of the surface is below the ignition wire. The ignition occurs on the left side of the cell causing a slosh to the right with a rapid drop of the liquid on the left. This sequence shows the surface as being characterized by additional smaller irregularities. The burn progresses in an asymmetric fashion predominantly along one side of the cell. Small waves move over the burning surface as is shown in the last frame.

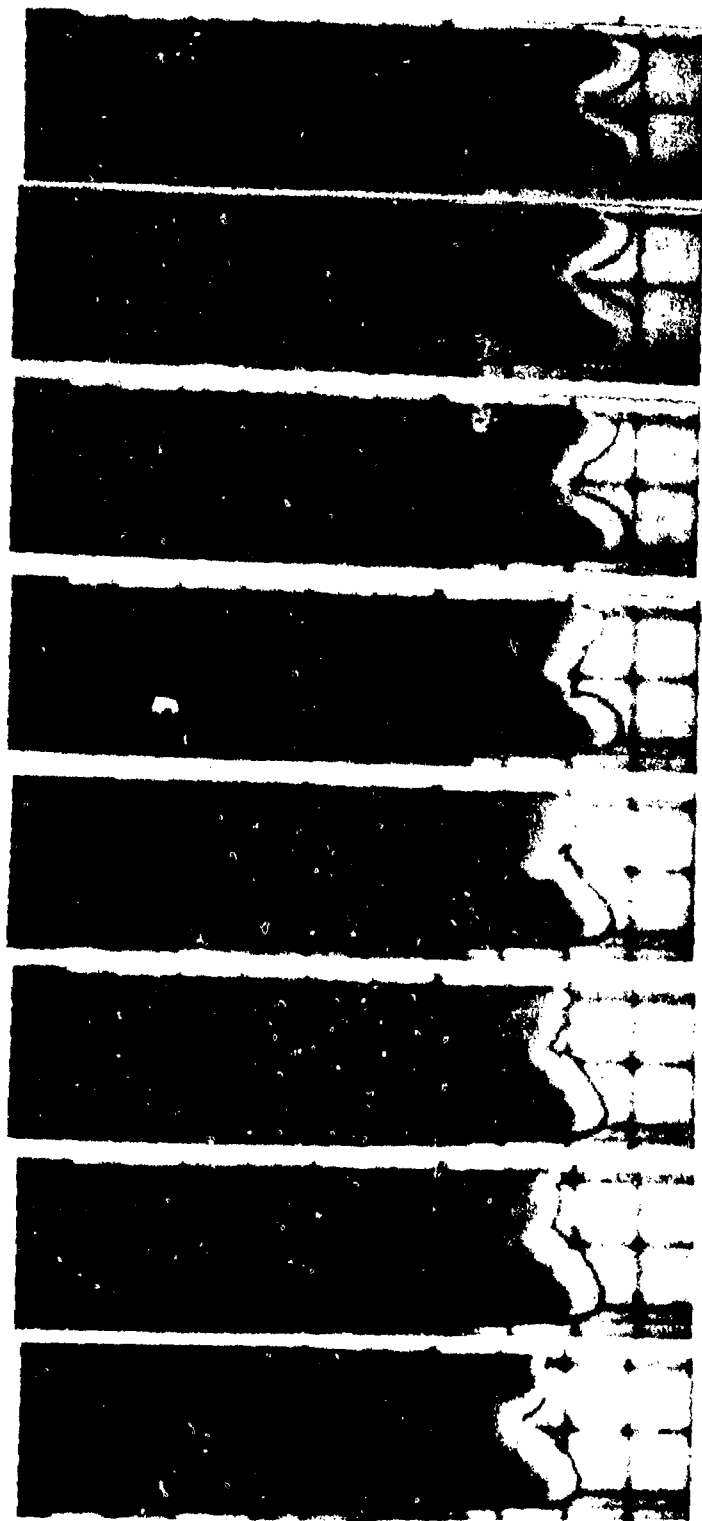
Figure 18, OTTO Fuel II, 6.1 x 1.5, Acrylic, 156 MPa: Ignition by use of a strip of M8 propellant did not give an initially flat surface due to asymmetric ignition of the M8 strip. This provided a slightly early LP ignition on the right of the cell and initiates some waves across the surface. The depression near the right wall grows at a high rate as at 129 MPa. As the dimensions of this depression increase the velocity of the tip decreases and small waves travel across this surface. They appear to be similar to the small surface waves observed in the NOSET "A" run at 70 MPa.

Observation of one of the small surface waves generated near the center line shows this peak dividing into two and separating with the generation of a depression between them. Apparently, the small ridge-like wave provides a locally high mass burn rate which provides a driving mechanism to depress the ridge-like structure and drive waves away from the area. The area under the former ridge can develop as a major depression.

4. Results. Table II and Figure 19 show the numerical data obtained photographically for OTTO Fuel II. Reference lines for OTTO Fuel II taken from Reference 1 are plotted in Figure 19 for comparison.

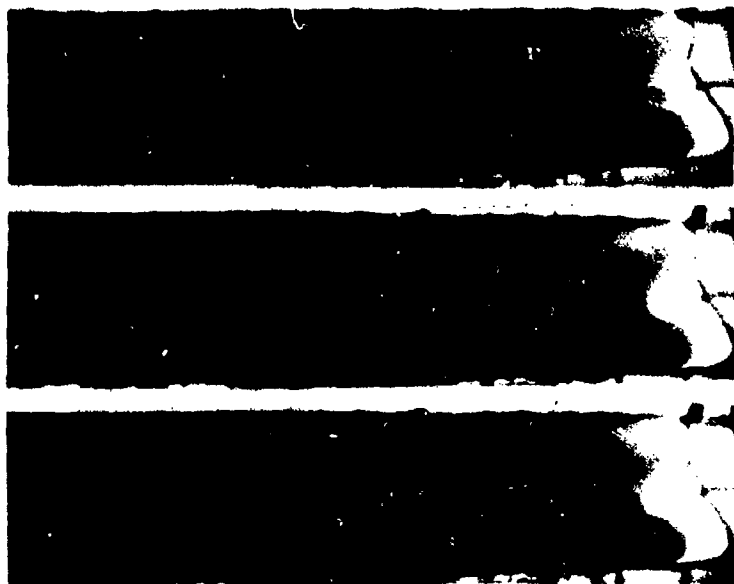
The higher values obtained at low pressures in the glass cells may be partly explained by a larger surface tension meniscus obtained in glass cells.

The high values obtained at the higher pressure are, by inspection of the plates, for strongly non-planar, non-steady surfaces. No attempt has been made to estimate a correction factor for the large surface area.

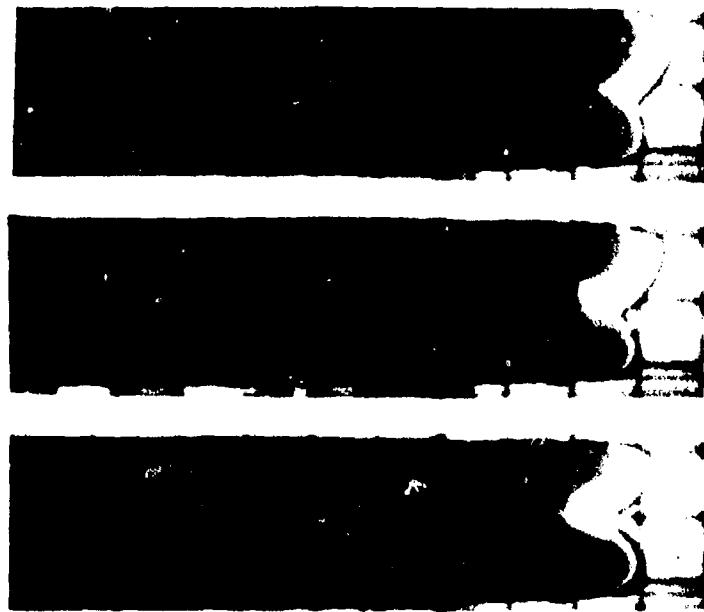


$\Delta T = 3.6 \text{ ms}$

Figure 16. OTTO Fuel II, 6.0 x 1.5 mm Acrylic Cell, 82.7 MPa



$\Delta T = 1.8 \text{ ms}$



$\Delta T = 3.6 \text{ ms}$

Figure 16. OTTO Fuel II, 6.0 x 1.5 mm Acrylic Cell, 82.7 MPa (Cont'd)



$\Delta T = 1.8 \text{ ms}$

Figure 17. OTTO Fuel II, 6.1 x 1.5 mm Acrylic Cell, 129 MPa



LATER



$\Delta T = 1.8 \text{ ms}$

Figure 17. OTTO Fuel II, 6.1 x 1.5 mm Acrylic Cell, 129 MPa (Cont'd)



Figure 18. OTTO Fuel II, 6.1 x 1.5 mm Acrylic Cell, 156 MPa

Table II. OTTO Fuel II Not Gelled

<u>P</u>	<u>W</u>	<u>C E L L</u>		<u>R</u>
<u>MPa</u>	<u>mm</u>	<u>T</u>	<u>MATERIAL</u>	<u>cm/s</u>
5.6	6.0	.95	Glass	.195
7.0	6.0	.95	Glass	.231
9.2	6.0	.95	Glass	.276
9.7	6.0	.95	Glass	.265
12.6	6.0	.95	Glass	.332
20.1	6.0	.95	Glass	.360
46.9	6.0	.95	Glass	1.92
60.0	6.0	.95	Glass	3.73
10.3	6.1	1.5	Acrylic	.231
82.7	6.1	1.5	Acrylic	5.08
128.0	6.1	1.5	Acrylic	8.21
156.0	6.1	1.5	Acrylic	9.4

NOTE: Estimated reading errors of 1% to 5% are to be expected from the photographic data. This is dependent upon the photographic quality and the nature of the surface.

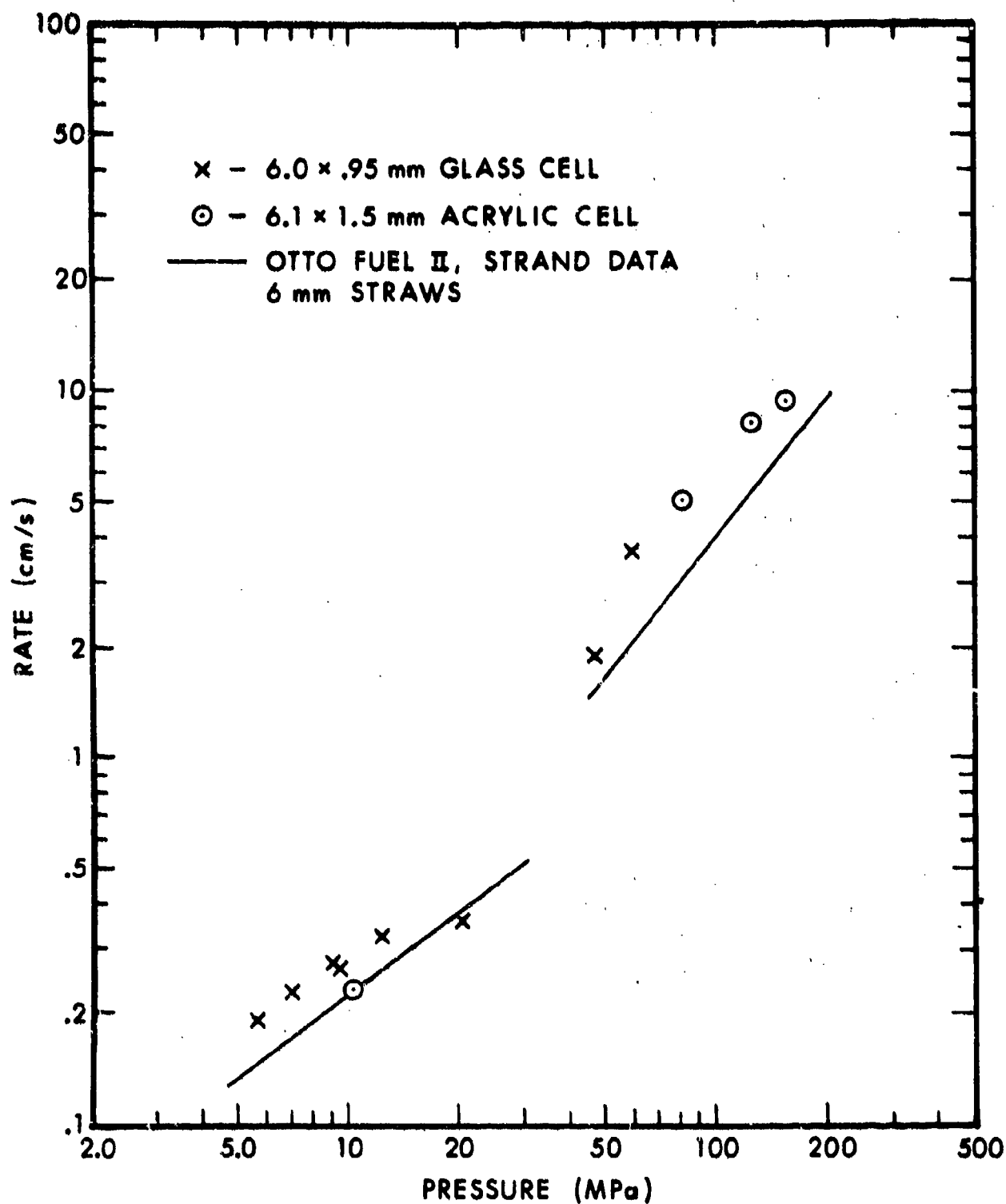


Figure 19. Burn Rates for OTTO Fuel II

Further work on ignition techniques and cell material interactions may clarify the causes for the disparity in the data at high pressures.

F. NOSET "A"

Figure 20 (20 MPa), 6.0 x .95 mm glass: The sequence of frames in Figure 20 clearly shows the wave action of the liquid. The initial frame shows the start of the sequence with a maximum meniscus to the left side and the wave minimum to the left. As the sequence progresses the liquid moves back up eliminating the meniscus and showing the start of a positive wave amplitude. In this sequence as the positive wave is formed a bubble is formed in the peak region and grows. The bubble finally breaks, scattering liquid into the gas and leaves streamers of liquid projecting up. As the upsurge proceeds, additional bubbles are formed and ruptured. The frames in this sequence show the same effects being started along the right of the cell. The formation of the bubbles may be due to the collection of heated propellant in the region of the peak, giving rise to ignition below the surface. The glass is apparently not getting hot enough at this pressure to ignite the sides of the propellant, as the rising portion of the wave covers glass that has been previously exposed.

Figure 21 (69.6 MPa), 6.0 x 1.5 mm, acrylic: This sequence shows a relatively stable general shape for the non-planar burn front. The "sloshing" observed at lower pressures is not evident. Also the shape is asymmetric relative to the cell. Small waves propagate over the larger surface and proceed up along the higher sides of the front. At the top of the large shape a streamer (or jet) is formed by the smaller waves.

The velocity of the lowest point is approximately 20 percent larger than the value obtained for the 6 mm straw samples in the standard strand burner tests.

V. CONCLUSIONS

The low thermal output of NOS-365 at lower pressures causes an erratic melting of the straw and will cause additional variability in the strand burner data for this propellant.

The agreement of the data of Figure 9 above 100 MPa, implies that this data from Reference 1 is for reasonably planar combustion.

The lower pressure data for the gelled NOS-365 must be corrected for the characteristic non-planarity observed in these tests.

The presence of a stable surface curvature in the lower pressure tests on OTTO Fuel II means that the lower pressure data of Reference 1

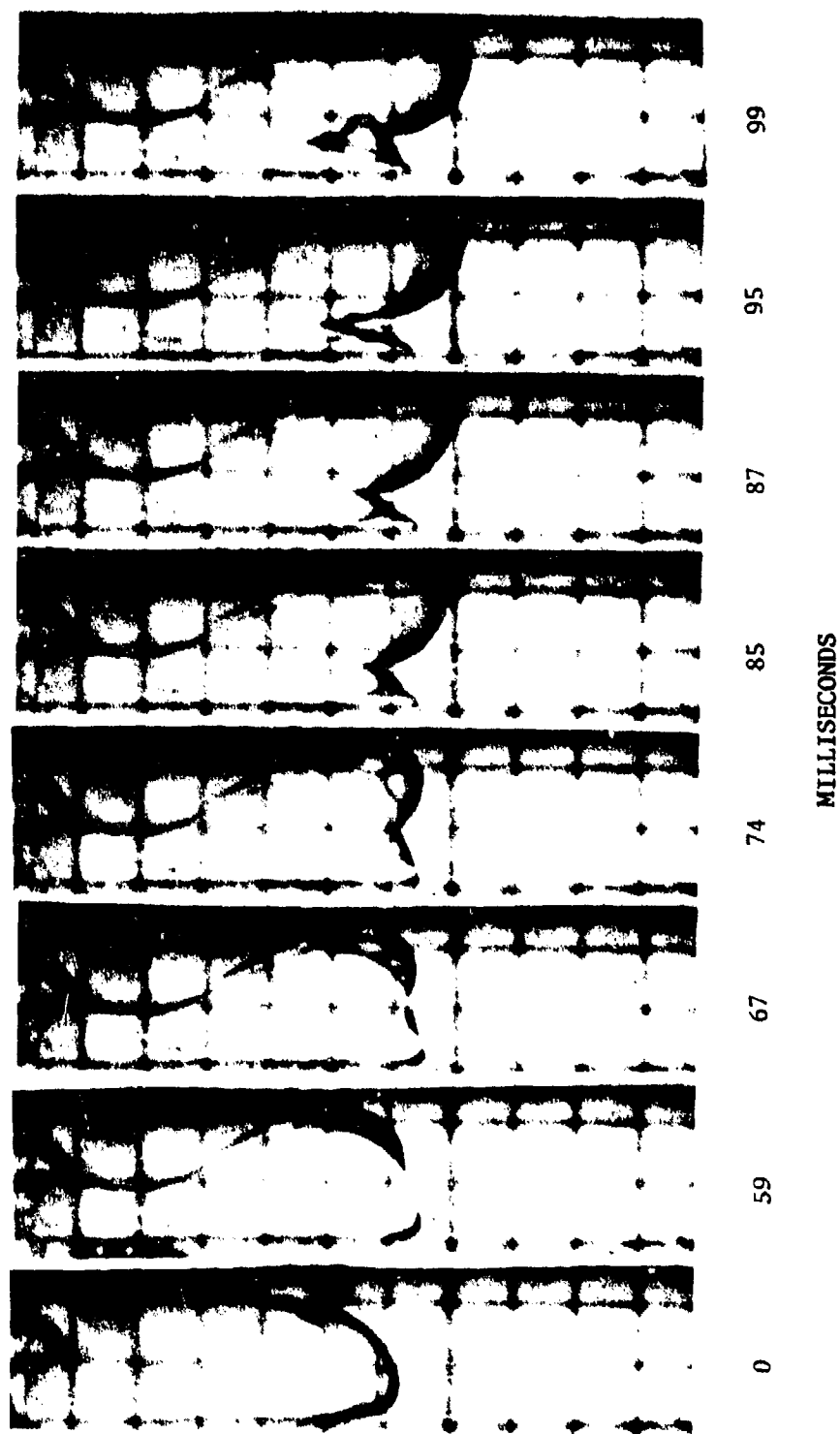
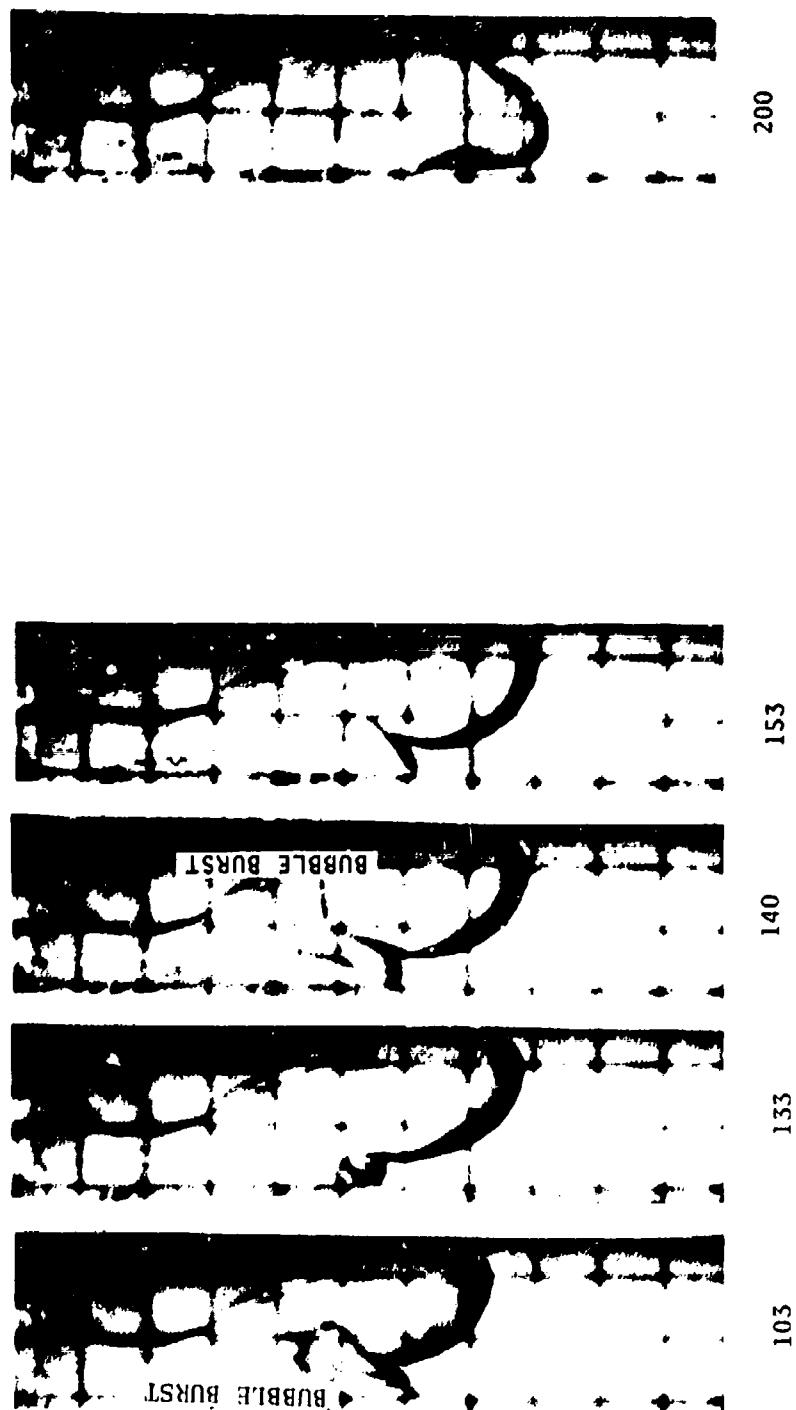
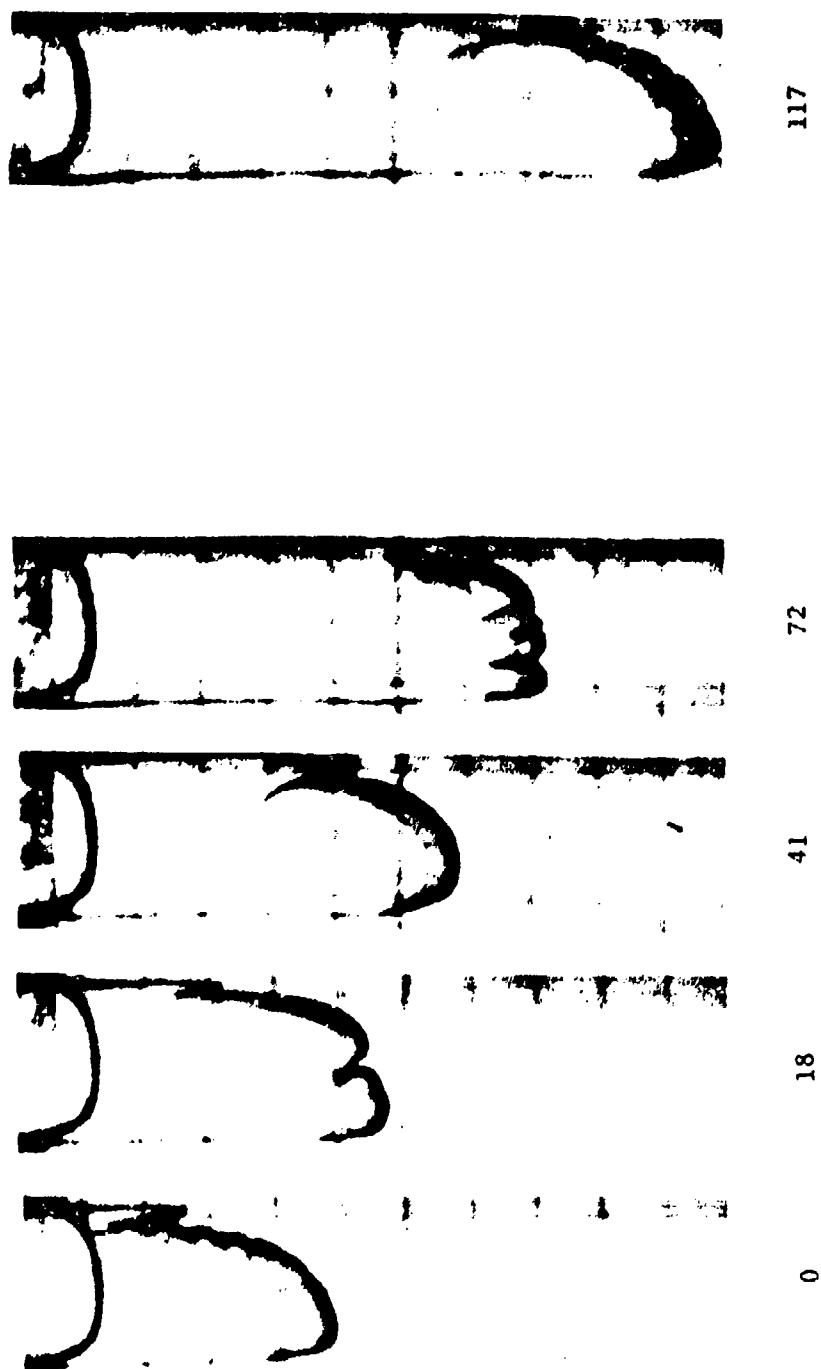


Figure 20. NOSET "A", 6.0 x .95 mm Glass Cell, 20 MPa



MILLISECONDS

Figure 20. NOSET "A", 6.0 x .95 mm Glass Cell, 20 MPa (Cont'd)



MILLISECONDS

Figure 21. NOSET "A", 6.0 x 1.5 mm Acrylic Cell, 69.6 MPa

may be slightly in error. Calculations based on surface area estimates from the photographic data indicate that it is reasonably accurate, however, further tests should be performed, directed at determining the extent of surface tension effects. A stable curved surface implies that liquid is being moved to maintain the shape, thus increasing the mass burn rate. Without liquid motion the surface should become flat due to burn-off.

The higher pressure data for OTTO Fuel II obtained in these tests has been so strongly non-planar that it is not especially helpful in determining the accuracy of the referenced data.

The tests that have been conducted on NOSET "A" show this propellant to be very useful as a photographic subject for this type of test. The clarity of detail with minimal obscuration makes this propellant a good candidate for studying the surface details.

DISTRIBUTION LIST

<u>No. of</u> <u>Copies</u>	<u>Organization</u>	<u>No. of</u> <u>Copies</u>	<u>Organization</u>
12	Commander Defense Technical Info Center ATTN: DDC-DDA Cameron Station Alexandria, VA 22314	3	Commander US Army Armament Research and Development Command Benet Weapons Laboratory ATTN: DRDAR-LCB-TL R. Hasenbein P. Votis Watervliet, NY 12189
1	Director Defense Advanced Research Projects Agency ATTN: LTC C. Buck 1400 Wilson Boulevard Arlington, VA 22209	1	Commander US Army Armament Materiel Readiness Command ATTN: DRSAR-LEP-L, Tech Lib Rock Island, IL 61299
1	HQDA (DAMA, C. Church) Washington, DC 20310	1	Commander US Army Aviation Research and Development Command ATTN: DRSAR-E 12th and Spruce Streets St. Louis, MO 63166
1	Commander US Army Materiel Development and Readiness Command ATTN: DRCMD-ST 5001 Eisenhower Avenue Alexandria, VA 22333	1	Director US Army Air Mobility Research and Development Laboratory Ames Research Center Moffett Field, CA 94035
5	Commander US Army Armament Research and Development Command ATTN: DRDAR-TSS (2) H. Fair, DRDAR-LC J.P. Picard, DRDAR-LC D. Downs, DRDAR-LC Dover, NJ 07801	1	Commander US Army Communications Research and Development Command ATTN: DRDCO-PPA-SA Fort Monmouth, NJ 07703
5	Commander US Army Armament Research and Development Command ATTN: W.L. Quine, DRDAR-LC A.J. Beardell, DRDAR-LC J. Hershkowitz, DRDAR-LC N. Slagg, DRDAR-LC M. Devine, DRDAR-SC Dover, NJ 07801	1	Commander US Army Electronics Research and Development Command Technical Support Activity ATTN: DELSD-L Fort Monmouth, NJ 07703
		1	Commander US Army Harry Diamond Labs ATTN: DRXDO-TI 2800 Powder Mill Road Adelphi, MD 20783

DISTRIBUTION LIST

<u>No. of Copies</u>	<u>Organization</u>	<u>No. of Copies</u>	<u>Organization</u>
2	Commander US Army Missile Command ATTN: DRDMI-R DRDMI-YDL Redstone Arsenal, AL 35809	2	Commander Naval Surface Weapons Center ATTN: O. Dengel K. Thorsted Silver Spring, MD 20910
2	Commander US Army Mobility Equipment Research and Development Cmd ATTN: DRDME-WC DRSME-RZT Fort Belvoir, VA 22060	3	Commander Naval Weapons Center ATTN: S. Wood L. Liedtke China Lake, CA 93555
1	Commander US Army Tank Automotive Research and Development Cmd ATTN: DRDTA-UL Warren, MI 48090	1	Commander Naval Ordnance Laboratory ATTN: K. Mueller Indian Head, MD 20640
1	Director US Army TRADOC Systems Analysis Activity ATTN: ATAA-SL(Tech Lib) White Sands Missile Range NM 88002	1	Superintendent Naval Postgraduate School ATTN: T. Houlihan Monterey, CA 93940
1	Office of the Chief of Naval Operations ATTN: Code NOP-351G Washington, DC 20360	1	Commander Naval Ordnance Station ATTN: G. Poudrier Indian Head, MD 20640
2	Commander Naval Sea Systems Command ATTN: SEA-55GH SEA-0331, J. Murrin Washington, DC 20360	1	AFOSR/NA, L. Caveny Bldg 41C Bolling AFB, DC 20332
2	Commander Naval Surface Weapons Center ATTN: W.C. Wieland T. Tschirn Dahlgren, VA 22448	2	AFATL/ATWG, O. Heiney DLD, D. Davis Eglin AFB, FL 32542
		1	Guns Test Branch AD 3246 TESTW/TETFG Eglin AFB, FL 32542
		2	US Bureau of Mines ATTN: R.A. Watson 4800 Forbes Street Pittsburgh, PA 15213

DISTRIBUTION LIST

<u>No. of</u> <u>Copies</u>	<u>Organization</u>	<u>No. of</u> <u>Copies</u>	<u>Organization</u>
1	Director Los Alamos Scientific Laboratory ATTN: D. Butler P.O. Box 1663 Los Alamos, NM 87545	2	General Electric Company Armament Systems Department ATTN: E. Ashley M. Bulman Burlington, VT 05401
1	Director Jet Propulsion Laboratory ATTN: Tech Lib 4800 Oak Grove Drive Pasadena, CA 91103	1	Mechanical Technology, Inc. ATTN: A. Graham 968 Albany-Shakes Road Lathan, NY 12110
2	Director National Aeronautics and Space Administration ATTN: MS-603, Tech Lib MS-86, Dr. Povinelli 21000 Brookpark Road Lewis Research Center Cleveland, OH 44135	1	Pulsepower Systems, Inc. ATTN: L.C. Elmore 815 American Street San Carlos, CA 93555
1	Director National Aeronautics and Space Administration Manned Spacecraft Center Houston, TX 77058	1	Science Applications, Inc. ATTN: R. Edelman 23146 Cumorah Crest Woodland Hills, CA 91364
1	Calspan Corporation ATTN: E. Fisher P.O. Box 235 Buffalo, NY 14221	1	Shock Hydrodynamics ATTN: W. Anderson 4710-16 Wineland Avenue N. Hollywood, CA 91602
1	Food & Machinery Corporation Norther Ordnance Division ATTN: J. Oberg Columbia Heights Post Office Minneapolis, MN 55421	1	TRW Systems ATTN: RI-1032, E. Fishman 1 Space Park Redondo Beach, CA 90278
4	General Electric Ordnance Dept ATTN: J. Haskins J. Mandzy R.E. Mayer H. West 100 Plastics Avenue Pittsfield, MA 01201	1	Director Applied Physics Laboratory The Johns Hopkins University Johns Hopkins Road Laurel, MD 20810
		2	Director Chemical Propulsion Info Agcy The Johns Hopkins University ATTN: T. Christian Tech Lib Johns Hopkins Road Laurel, MD 20810

DISTRIBUTION LIST

<u>No. of Copies</u>	<u>Organization</u>	<u>No. of Copies</u>	<u>Organization</u>
1	Director Graduate Center of Applied Science New York University ATTN: M. Summerfield 26-36 Stuyvesant New York, NY 10003	1	SRI International ATTN: Code L3106, G.A. Branch 333 Ravenswood Avenue Menlo Park, CA 94025
1	Pennsylvania State University Applied Research Laboratory ATTN: K. Kuo University Park, PA 16802	1	University of Mississippi Mechanical Engineering Dept ATTN: C.R. Wimberly University, MS 38677
1	Princeton University Department of Aerospace and Mechanical Sciences ATTN: Tech Lib James Forrestal Campus Princeton, NJ 08540		<u>Aberdeen Proving Ground</u> Dir, USAMSAA ATTN: DRXSY-D DRXSY-MP, H. Cohen Cdr, USATECOM ATTN: DRSTE-TO-F Dir, Wpns Sys Concepts Team Bldg E3516, EA ATTN: DRDAR-ACW

USER EVALUATION OF REPORT

Please take a few minutes to answer the questions below; tear out this sheet and return it to Director, US Army Ballistic Research Laboratory, ARRADCOM, ATTN: DRDAR-TSB, Aberdeen Proving Ground, Maryland 21005. Your comments will provide us with information for improving future reports.

1. BRL Report Number _____
2. Does this report satisfy a need? (Comment on purpose, related project, or other area of interest for which report will be used.)

3. How, specifically, is the report being used? (Information source, design data or procedure, management procedure, source of ideas, etc.) _____

4. Has the information in this report led to any quantitative savings as far as man-hours/contract dollars saved, operating costs avoided, efficiencies achieved, etc.? If so, please elaborate.

5. General Comments (Indicate what you think should be changed to make this report and future reports of this type more responsive to your needs, more usable, improve readability, etc.) _____

6. If you would like to be contacted by the personnel who prepared this report to raise specific questions or discuss the topic, please fill in the following information.

Name: _____

Telephone Number: _____

Organization Address: _____

